

# High Speed Two-Photon Lifetime Imaging

Sebastian Karpf\* and Bahram Jalali

\*corresponding author: nino.karpf@gmail.com

## Abstract

Nonlinear optical techniques and in particular two photon excited fluorescence imaging<sup>1</sup> have emerged as powerful tools for deep tissue imaging with subcellular resolution<sup>2</sup>, brain mapping<sup>3</sup> and 3D printing<sup>4</sup>. At the same time, fluorescent lifetime imaging<sup>5</sup> probes internal biochemical interactions and external environment of a molecule useful for DNA sequencing<sup>6</sup>, detection of tumour margins necessary for successful surgical removal<sup>7</sup>, and quantifying cellular energy metabolism in living cells<sup>8</sup>. To image fast dynamic processes such as biological cells in flow or neural activities, these methods must provide frame rates beyond 1000Hz. However, achieving high speed is challenged by lower efficiency of nonlinear vs. linear processes requiring illumination with a high-intensity tightly-focused beam that is scanned over sample area. The scanning is typically done with mechanical scanners the speed of which limits the frame rate. Acousto-optic scanners<sup>9</sup> provide an intermediate solution however the frame rate is limited by the acoustic velocity leading to a trade-off between resolution and speed. Here we report on a new tool for high-speed non-linear imaging and demonstrate its utility in two photon fluorescence<sup>1</sup> and fluorescence lifetime imaging (FLIM)<sup>5</sup>. A rapidly wavelength-swept Fourier-Domain Mode-Locked (FDML)<sup>10</sup> laser with digitally synthesized electro-optic modulation in a master oscillator-power amplifier configuration is combined with spectral encoding to eliminate the speed limitations of inertial scanning and achieve single-shot imaging. We demonstrate lifetime imaging with 2kHz frame-rate (88MHz pixel rate) – a record for both FLIM and two-photon FLIM. To the best of our knowledge, this is the first report of spectrally encoded multiphoton imaging. We also show optical image compression via spatially-warped two photon excitation and scale invariant digital zoom. This method allows nonlinear imaging flow cytometry, rapid recording of neuronal activity and mapping non-repetitive biomolecular dynamics at a sub-cellular optical resolution. Being fibre based this method has the potential for endoscopic medical applications.

## Main

## Introduction

Two Photon Microscopy<sup>1</sup> enables deep tissue imaging at high resolution. Since its introduction, a main interest of research has been increasing the imaging speed above 1kHz in order to observe millisecond dynamics of neural activity<sup>11</sup> and to avoid artefacts in a moving target. In Two-Photon Microscopy, the required excitation power depends on illumination intensity squared. This quadratic dependency favours beam-steering over wide-field illumination leading to the popular use of galvanometric scanning mirrors. Such mechanically scanning mirrors are inertia-limited and too slow for 2-D frame-rates in the biologically important kHz range. Fast imaging speeds are also desired for superior signal generation performance<sup>12-14</sup>.

Different approaches for overcoming the inertia-limit of mechanical scanners have been investigated, with the most prominent employing either acousto-optic deflectors (AOD)<sup>9,13</sup> or parallelizing the

excitation by employing multiple beams<sup>15-17</sup>. However, these approaches have added complexity, require for dispersion management and lack high timing resolution. The finite latency associated with the propagation velocity of the acoustic wave through the acousto-optic interaction volume causes an ambiguity in the diffraction angle leading to reduced spatial resolution at high scanning rates. This trade-off between resolution and speed is a fundamental known limitation of AOD technology<sup>16</sup>. Also, it is difficult to augment AOD scanning with fibre delivery which is crucial for endoscopic applications.

Spectral-Encoded scanning increases imaging speeds by spectrum-to-space mapping and has been employed for confocal microscopy<sup>18</sup>. Photonic time stretch is a high speed data acquisition method<sup>19</sup> that combined with spectral scanning leads to single shot acquisition of bright field images with record speed<sup>20</sup>. Interferometric time stretch achieving fast phase sensitive imaging has been combined with artificial intelligence for successful label-free classification of cancer cells in blood in a microfluidic channel<sup>21</sup>. In time stretch microscopy, both the spectrum and the time are needed to identify the pixel location through spectrum to time mapping. Extension of time stretch to fluorescence imaging has been hindered because both the emission spectrum and fluorescent lifetime are governed by the molecule which is independent of spectrum-to-time mapping.

To enable fast fluorescent imaging, we introduced the radio frequency (RF) encoded excitation (FIRE) technique<sup>22</sup>. The RF domain was utilized instead of the optical spectrum for spatial encoding enabling multi-KHz frame rate single photon fluorescent imaging<sup>22</sup>. The technique can also perform rapid single-pixel lifetime measurements<sup>23</sup> but not rapid lifetime imaging. Extension of FIRE to two photon imaging<sup>24</sup> is difficult because an entire line scan is illuminated simultaneously resulting in insufficient optical intensity for excitation of two photon processes.

### **Our solution – general description**

To enable fast two photon fluorescent imaging with simultaneous lifetime imaging, here we introduce Two-Photon Spectro-temporal Lifetime Imaging by Digitally sculpted Excitation (SLIDE). This technique independently detects the location, the amplitude and the lifetime of fluorescent emission - a feat that has not been achieved with previous spectral and RF-encoding and time stretch technique. We accomplish this by synthesizing a sequential excitation beam via digital electro-optic modulation of a quasi-CW swept source followed by time encoded detection (cf. Fig. 1). To enable fluorescent imaging, spectral and temporal mappings are employed separately, with quasi-CW spectral encoding used for pumping and time encoding for constructing the image at fluorescence wavelength.

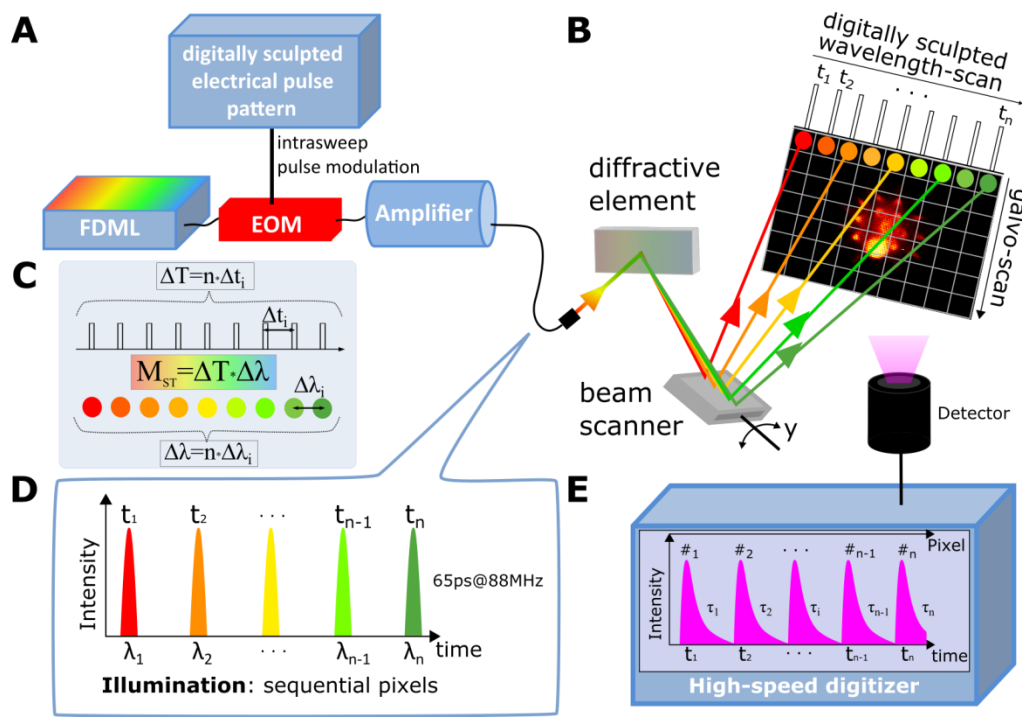


**Figure 1 Principle of Spectro-temporal Lifetime Imaging by digitally sculpted excitation (SLIDE).** (A) A swept-source Fourier Domain Mode-Locked (FDML) laser is pulse-modulated, amplified and diffracted to produce rapid beam steering through spectrum-to-line mapping (B). The mapping pattern is digitally sculpted through the pulse modulation. The y-axis is scanned by a beam scanner. (C) The FDML laser provides a high spectro-temporal bandwidth  $M_{ST}$ . This figure of merit is the product of the spectral span ( $\Delta\lambda$ ) required for high-resolution imaging and the line-scan speed  $\Delta T$ , which is governed by the fluorescence decay times and the pixel number. (D) In SLIDE, each pulse has both a unique wavelength and time leading to a sequential and pixelwise illumination. (E) After fluorescence excitation, this mapping allows both straightforward image generation and even recording of the fluorescent lifetimes using a high-speed digitizer. Typical excitation pulse length is 65ps at 88MHz repetition rate with peak power ranging from 1.8-18W and average power 10-100mW (pulse energies of 0.12-1.2nJ).

Spectro-temporal Lifetime Imaging places rigorous requirements on the time-bandwidth of the optical source requiring tens of nanometers wavelength sweep in a few microseconds with a product that increases quadratically with the number of pixels (see Methods section). Fourier domain Mode locked<sup>10</sup> (FDML) lasers provide such a performance. In the SLIDE system, the laser is pulse-modulated by an electro-optic modulator (EOM, Fig.1) generating 65ps pulses and amplified to high instantaneous powers sufficient for two photon excitation. Upon spatial diffraction, spectrally swept pulses (Fig. 1D) pump the sample with a unique spatial and temporal sequence (Fig. 1B). The EOM modulation leads to digitally sculpted waveforms making the excitation pattern digitally programmable. Digitally temporal synthesis (Fig.1D) assigns a unique timing to each pixel. The image is constructed from the time of arrival of the fluorescence signal which is recorded in epi-direction on a hybrid photodetector, digitized and processed on a computer.

Spectro-temporal imaging with large spectro-temporal bandwidth permits simultaneous single shot Two-Photon excited fluorescence (TPEF) and fluorescence lifetime imaging (2P-FLIM)<sup>25</sup>. The current standard for fluorescent lifetime measurement is time-correlated single-photon counting (TCSPC). Its inherent drawback is the speed limitation caused by less than one fluorescence photon emission per excitation pulse. The system reported by us is several orders of magnitude faster.

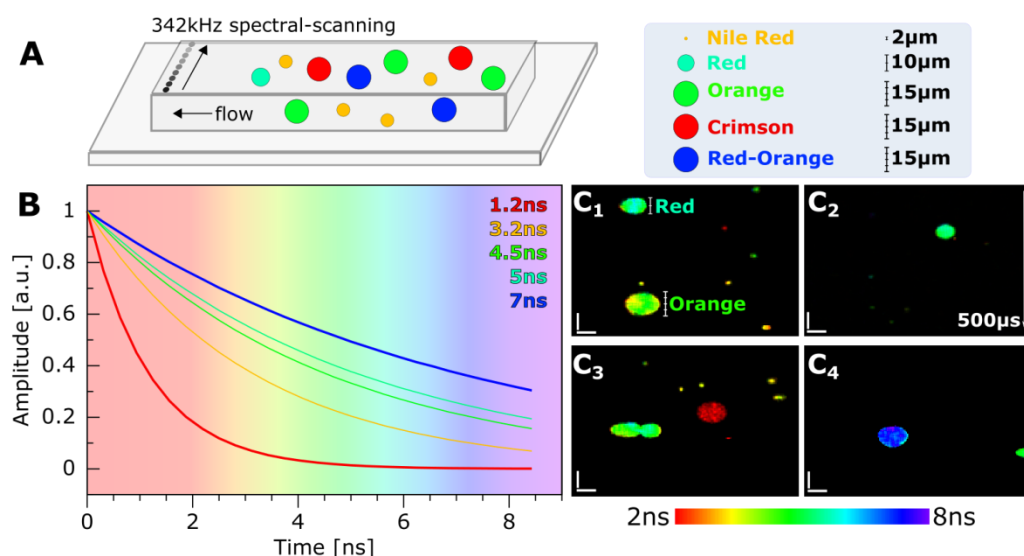


**Figure 2** Two-Photon Fluorescence Lifetime Imaging (2P-FLIM) in high-speed flow-cytometry. (A) The vertical axis was scanned by the SLIDE swept laser scan at 342 kHz line-scanning rate. At 550nm resolution sampling, the imaging flow-rate was 0.2m/s. Five different species of blood-flow determination fluorescent beads were imaged and colour-coded based on their fluorescent lifetime. The images clearly show the five different species. (B) The fitted lifetimes of the Crimson (red), Nile Red (yellow) and Red-Orange (blue) beads are clearly distinguishable. Each lifetime curve is taken from a single pixel after a 9x9 box blur filter was applied. The lifetimes of the Red and Orange beads lie very close together and can hardly be distinguished by mere lifetime (C<sub>1</sub>). However, their different sizes of 10μm and 15μm, respectively, are clearly resolved in the lifetime images (C<sub>1</sub>). Each line was scanned at 2.92μs, so for a 256x170 image the recording time is only 497μs (C<sub>1</sub>-C<sub>4</sub>). The pixel rate was 88MHz, i.e. single excitation pulse per pixel without averaging. The power used was 15mW, scale bars represent 10μm. The high-throughput and the combination of different, independent physical information (morphology, fluorescence, lifetime etc.) could in the future be applied to targeted detection of e.g. rare tumour cells in blood<sup>26</sup> or rapid cell sorting at high specificity by intelligently analyzing the features with artificial intelligence and machine learning<sup>21</sup>.

For cell classification and detection of rare cells, such as circulating tumour and fetal cells, it is important to measure a high number of cells quickly, accurately and as non-invasively as possible. Two-photon microscopy has high three dimensional resolution, can operate in blood flow<sup>26</sup> and offers deeper penetration than one-photon techniques through the use of longer wavelengths.

To showcase the system's capabilities, we first show in Figure 2 2P-FLIM based flow cytometry at 88MHz pixel rate. The particles are fluorescent beads used in blood flow determination studies with diameters in the range 2-15μm, similar to typical cell sizes. The flow-rate was set to 0.2m/s, limited by diffraction spot size and fluorescent lifetime (see methods). Two photon imaging in flow has potential for non-invasive *in vivo* cancer cell detection through the skin barrier<sup>26</sup>.

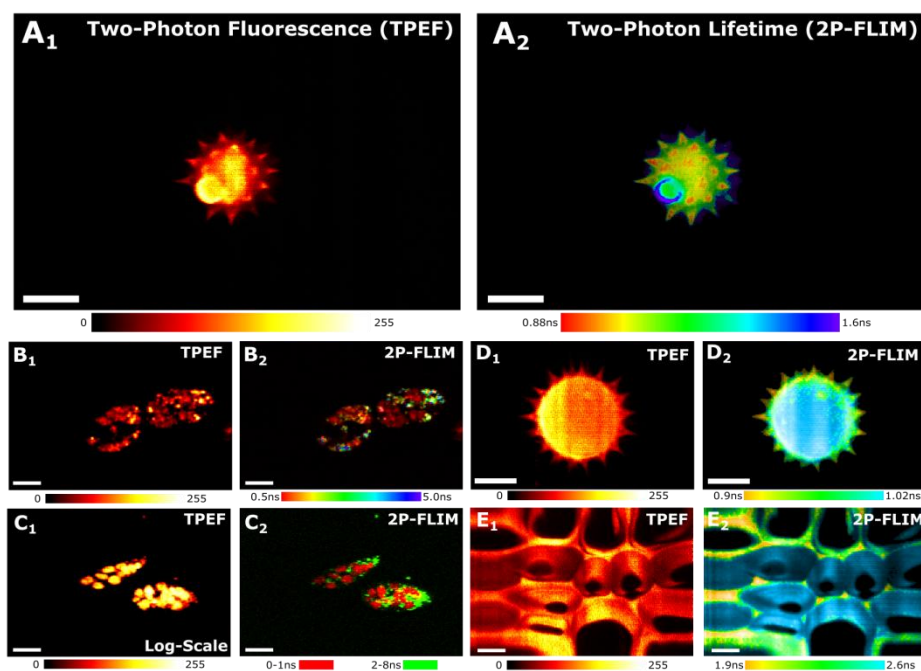


Figure 3 Dual-Modality Images obtained with the SLIDE imaging approach. (A<sub>1</sub>) Two-Photon excited fluorescence (TPEF) image of a Pollen grain. Image size is 512x340 px, pixel-rate 176MHz, 100-times averaged, 80mW on the sample. (A<sub>2</sub>) A Two-Photon fluorescence lifetime image (2P-FLIM) is generated from the same data by fitting an exponential decay to the analogue fluorescence decay curve. The autofluorescence reveals different lifetimes for the body and the spikes, which is not visible in the mere TPEF image. (B<sub>1</sub>) A *Euglena gracilis* algae whose chloroplasts provide autofluorescence while the lipids were stained with Nile Red. The unaveraged image consists of 256x170 pixels and was acquired within 497  $\mu$ s (2 kHz frame-rate, 30mW optical power). (B<sub>2</sub>) 2P-FLIM image of the Euglena clearly shows the difference in lifetime between the chlorophyll (red) and the Nile Red stained lipids (green-blue). (C<sub>1</sub>) Euglena TPEF image on a logarithmic scale shows high SNR (100 avg, 60mW), but different cellular compartments are indistinguishable. (C<sub>2</sub>) Computationally fast integration of 0-1ns (red) and 2-8 ns (green) time windows, however, reveal clear lifetime differences. (D<sub>1</sub>) Pollen grain (100-avg) with sub-micron features is clearly resolved demonstrating the high-resolution of the SLIDE setup. (D<sub>2</sub>) 2P-FLIM image of the Pollen grain. (E<sub>1</sub>) Acridine Orange stained *convallaria majalis* sample (100 avg, 80mW). (E<sub>2</sub>) 2P-FLIM reveals differences in fluorescence lifetime based on the molecular environment inside the sample. For all 2P-FLIM images, a 3x3 box blur filter was applied in the time-domain (see methods). Scale bar represents 10 $\mu$ m (see methods).

Figure 3 shows a mix of high speed two photon fluorescent and fluorescent lifetime images. Fig. 3A was recorded at 176 MHz pixel rate for 512x340 pixels and a frame-rate of 1kHz. For high SNR, 100 frames were averaged. Figures 3B-E consists of 256x170 pixel frames, corresponding to a pixel-rate of 88MHz and a frame-rate of 2kHz.

Fluorescent imaging can be used for classifications of algae cells used in biofuels based on their lipid content. Fig. 3B<sub>1</sub> shows *Euglena gracilis* algae cells with rich lipid content stained with Nile Red. The cell's chloroplasts provide endogenous autofluorescence and the difference in fluorescent lifetimes clearly highlight the different sub-cellular features (Fig. 3B<sub>2</sub>). These images are unaveraged and acquired within 497 $\mu$ s for both TPEF and 2P-FLIM images acquired simultaneously. The lifetimes were extracted by deconvolving with the instrument's response function (IRF, see methods). Fig. 3C<sub>1</sub> shows the same for another *Euglena gracilis* algae cell on a logarithmic scale to highlight faintest features. This TPEF image was 100-times averaged (20Hz acquisition rate). In the 2P-FLIM image (Fig. 3C<sub>2</sub>) the lifetime was mapped

into an RGB format (see Methods). Fig. 3D and E further demonstrate the high resolution capability of our technique where diffraction-limited features are clearly resolved.

Since the fluorescent excitation pattern can be digitally programmed it can adapt to the sample being imaged. In Figure 4 we present applications of this to foveated (non-uniform) sampling for image compression<sup>27</sup> and to digital zoom. By engineering the temporal pulse density, we adapt the excitation pixel density to the sparsity of the sample. Figures 4A-F show one example where high pixel resolution is achieved in the central field of view with lower density in the peripheral vision. As shown in Figures 4C and 4F, higher resolution by a factor 2.5 can be achieved with same number of pixels (see Methods for details). It is important to note that we achieve this through direct nonuniform sampling in contrast to warped (anamorphic) stretch of the image prior to uniform sampling as recently demonstrated<sup>27</sup>. In high-speed imaging, this optical data compression reduces the amount of data generated alleviating the digital processing and storage requirements.

In SLIDE, the excitation pattern can also be digitally sculpted through waveform controlling the wavelength sweep of the FDML laser. In Fig. 4G-I, we show digitally controlled optical zoom for TPEF and 2P-FLIM (see Methods). Unlike conventional digital zoom, here the resolution is not lost at high magnifications (Fig. 4G-I).

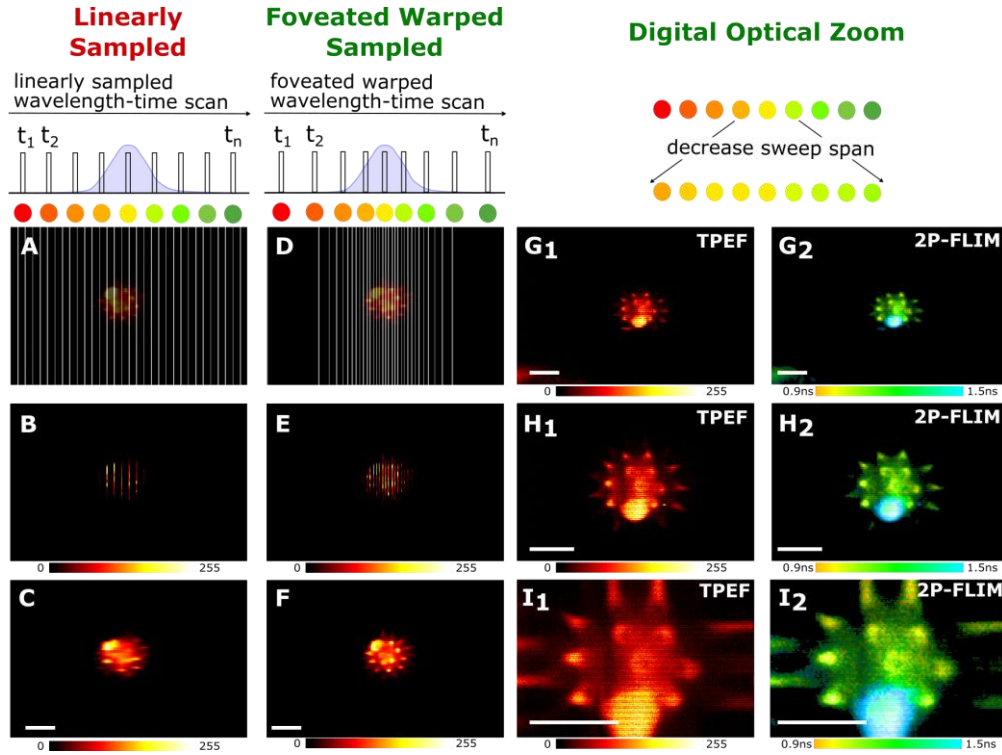


**Figure 4** Digitally sculpted waveforms enable flexible imaging parameters. (A-F) The horizontal pixel rate can be reduced to achieve lower average power, while keeping the frame-rate constant. A pixel rate of only 11MHz was programmed, corresponding to 32 Pixels per line, lowering the average power to 20mW. When using a linear sampling pattern (A), the sharp features of the Pollen grain are under-sampled (B). After interpolation the spikes of the Pollen grain are almost not visible (C). However, when programming a foveated warped sampling pattern (D), higher sampling density is allotted to the centre of the image (E). After interpolation, the Pollen grain can be nicely resolved even at only 32 horizontal pixels per line (F). The resolution enhancement in the centre is 2.5. Another capability is scale invariant digital optical zoom, which is achieved by digitally decreasing the sweep span of the FDML laser. The TPEF and 2P-FLIM images showing a high-detailed

Pollen grain ( $G_1, G_2$ ) can be more effectively sampled by reducing the spectral span 1.5-fold ( $H_1, H_2$ ) or 3-fold ( $I_1, I_2$ ) while maintaining the optical resolution. The scale bars represent 10 $\mu$ m.

It is important to discuss the power requirements for the SLIDE system. The high frame-rate introduced here requires about 3-10-times higher average powers than slower femtosecond laser based systems. This is a consequence of the faster imaging approach and the picosecond pulses and the powers are similar to multi-focus approaches. Advantageously, the longer pulses can generate a higher number of photons per fluorescence event<sup>25</sup> which lowers the relative shot-noise which can limit the SNR and thus the imaging speed in non-linear imaging<sup>28</sup>.

In summary, we have presented a new approach for fast fluorescent and fluorescent lifetime imaging and demonstrated record speed lifetime imaging in flow. Sculpting the illumination pattern through digitally synthesized spectro-temporal patterns, we demonstrated optical data compression and scale-invariant-resolution zoom functionality. The system operates around 1060nm offering reduced scattering and deep tissue imaging capability. Finally, the introduced FDML-MOPA laser is fibre-based which may lead to an endoscopic application for rapid TPEF and 2P-FLIM for *in vivo* and *in situ* biological imaging.

**Acknowledgement:** We would like to thank Dr. Carson Riche and Prof. Dino di Carlo from UCLA for providing the *Euglena gracilis* algae cells. This research was sponsored in part by the National Institutes of Health grants 5R21GM107924-03 and R21EB019645. Sebastian Karpf gratefully acknowledges a Postdoctoral research fellowship from the German Research Foundation (DFG, project KA 4354/1-1).

**Author Contributions:** S.K. conceived the system and conducted the experiment. S.K. and B.J. conceived the digital image processing capabilities. B.J. and S.K. performed system analysis and wrote the manuscript.

## Reference List

- 1 Denk, W., Strickler, J. & Webb, W. Two-photon laser scanning fluorescence microscopy. *Science* **248**, 73-76, doi:10.1126/science.2321027 (1990).
- 2 Theer, P., Hasan, M. T. & Denk, W. Two-photon imaging to a depth of 1000  $\mu$ m in living brains by use of a Ti:Al<sub>2</sub>O<sub>3</sub> regenerative amplifier. *Opt. Lett.* **28**, 1022-1024, doi:10.1364/OL.28.001022 (2003).
- 3 Svoboda, K. & Yasuda, R. Principles of Two-Photon Excitation Microscopy and Its Applications to Neuroscience. *Neuron* **50**, 823-839, doi:https://doi.org/10.1016/j.neuron.2006.05.019 (2006).
- 4 Haske, W. *et al.* 65 nm feature sizes using visible wavelength 3-D multiphoton lithography. *Opt. Express* **15**, 3426-3436, doi:10.1364/OE.15.003426 (2007).
- 5 Lakowicz, J. R., Szmacinski, H., Nowaczyk, K., Berndt, K. W. & Johnson, M. Fluorescence lifetime imaging. *Analytical Biochemistry* **202**, 316-330, doi:http://dx.doi.org/10.1016/0003-2697(92)90112-K (1992).
- 6 Neumann, M., Herten, D. P., Dietrich, A., Wolfrum, J. & Sauer, M. Capillary array scanner for time-resolved detection and identification of fluorescently labelled DNA fragments. *Journal of Chromatography A* **871**, 299-310, doi:https://doi.org/10.1016/S0021-9673(99)00909-7 (2000).
- 7 Cubeddu, R., Canti, G., Pifferi, A., Taroni, P. & Valentini, G. Fluorescence Lifetime Imaging of Experimental Tumors in Hematoporphyrin Derivative-Sensitized Mice. *Photochemistry and Photobiology* **66**, 229-236, doi:10.1111/j.1751-1097.1997.tb08648.x (1997).



- 8 Blacker, T. S. *et al.* Separating NADH and NADPH fluorescence in live cells and tissues using FLIM. *Nature Communications* **5**, 3936, doi:10.1038/ncomms4936 (2014).
- 9 Lechleiter, J. D., Lin, D.-T. & Sieneart, I. Multi-Photon Laser Scanning Microscopy Using an Acoustic Optical Deflector. *Biophysical Journal* **83**, 2292-2299, doi:http://dx.doi.org/10.1016/S0006-3495(02)73989-1 (2002).
- 10 Huber, R., Wojtkowski, M. & Fujimoto, J. G. Fourier Domain Mode Locking (FDML): A new laser operating regime and applications for optical coherence tomography. *Opt. Express* **14**, 3225-3237, doi:10.1364/OE.14.003225 (2006).
- 11 Gong, Y. *et al.* High-speed recording of neural spikes in awake mice and flies with a fluorescent voltage sensor. *Science* **350**, 1361-1366, doi:10.1126/science.aab0810 (2015).
- 12 Donnert, G., Eggeling, C. & Hell, S. W. Major signal increase in fluorescence microscopy through dark-state relaxation. *Nat Meth* **4**, 81-86 (2007).
- 13 Chen, X., Leischner, U., Rochefort, N. L., Nelken, I. & Konnerth, A. Functional mapping of single spines in cortical neurons in vivo. *Nature* **475**, 501-505, doi:http://www.nature.com/nature/journal/v475/n7357/abs/nature10193.html#supplementary-information (2011).
- 14 Chen, X. *et al.* LOTOS-based two-photon calcium imaging of dendritic spines in vivo. *Nat. Protocols* **7**, 1818-1829 (2012).
- 15 Bewersdorf, J., Pick, R. & Hell, S. W. Multifocal multiphoton microscopy. *Opt. Lett.* **23**, 655-657, doi:10.1364/OL.23.000655 (1998).
- 16 Kim, K. H. *et al.* Multifocal multiphoton microscopy based on multianode photomultiplier tubes. *Opt. Express* **15**, 11658-11678, doi:10.1364/OE.15.011658 (2007).
- 17 Cheng, A., Goncalves, J. T., Golshani, P., Arisaka, K. & Portera-Cailliau, C. Simultaneous two-photon calcium imaging at different depths with spatiotemporal multiplexing. *Nat Meth* **8**, 139-142, doi:http://www.nature.com/nmeth/journal/v8/n2/abs/nmeth.1552.html#supplementary-information (2011).
- 18 Tearney, G. J., Webb, R. H. & Bouma, B. E. Spectrally encoded confocal microscopy. *Opt. Lett.* **23**, 1152-1154, doi:10.1364/OL.23.001152 (1998).
- 19 Bhushan, A. S., Coppinger, F. & Jalali, B. Time-stretched analogue-to-digital conversion. *Electronics Letters* **34**, 839-841, doi:10.1049/el:19980629 (1998).
- 20 Goda, K., Tsia, K. K. & Jalali, B. Serial time-encoded amplified imaging for real-time observation of fast dynamic phenomena. *Nature* **458**, 1145-1149, doi:http://www.nature.com/nature/journal/v458/n7242/supinfo/nature07980\_S1.html (2009).
- 21 Chen, C. L. *et al.* Deep Learning in Label-free Cell Classification. *Scientific Reports* **6**, 21471, doi:http://dx.doi.org/10.1038/srep21471 (2016).
- 22 Diebold, E. D., Buckley, B. W., Gossett, D. R. & Jalali, B. Digitally synthesized beat frequency multiplexing for sub-millisecond fluorescence microscopy. *Nat Photon* **7**, 806-810, doi:http://www.nature.com/nphoton/journal/v7/n10/full/nphoton.2013.245.html (2013).
- 23 Chan, J. C. K. *et al.* Digitally synthesized beat frequency-multiplexed fluorescence lifetime spectroscopy. *Biomed. Opt. Express* **5**, 4428-4436, doi:10.1364/BOE.5.004428 (2014).
- 24 Tsyboulski, D., Orlova, N. & Saggau, P. Amplitude modulation of femtosecond laser pulses in the megahertz range for frequency-multiplexed two-photon imaging. *Opt. Express* **25**, 9435-9442, doi:10.1364/OE.25.009435 (2017).
- 25 Karpf, S. *et al.* Two-photon microscopy using fiber-based nanosecond excitation. *Biomed. Opt. Express* **7**, 2432-2440, doi:10.1364/BOE.7.002432 (2016).
- 26 He, W., Wang, H., Hartmann, L. C., Cheng, J.-X. & Low, P. S. In vivo quantitation of rare circulating tumor cells by multiphoton intravital flow cytometry. *Proceedings of the National Academy of Sciences* **104**, 11760-11765, doi:10.1073/pnas.0703875104 (2007).



- 27 Chen, C. L., Mahjoubfar, A. & Jalali, B. Optical Data Compression in Time Stretch Imaging. *PLOS ONE* **10**, e0125106, doi:10.1371/journal.pone.0125106 (2015).
- 28 Stoltzfus, C. R. & Rebane, A. Optimizing ultrafast illumination for multiphoton-excited fluorescence imaging. *Biomed. Opt. Express* **7**, 1768-1782, doi:10.1364/BOE.7.001768 (2016).
- 29 Klein, T. & Huber, R. High-speed OCT light sources and systems [Invited]. *Biomed. Opt. Express* **8**, 828-859, doi:10.1364/BOE.8.000828 (2017).
- 30 Wieser, W. *et al.* High definition live 3D-OCT in vivo: design and evaluation of a 4D OCT engine with 1 GVoxel/s. *Biomed. Opt. Express* **5**, 2963-2977, doi:10.1364/BOE.5.002963 (2014).
- 31 Eigenwillig, C. M. *et al.* Picosecond pulses from wavelength-swept continuous-wave Fourier domain mode-locked lasers. *Nat Commun* **4**, 1848, doi:10.1038/ncomms2870 (2013).
- 32 Karpf, S., Eibl, M., Wieser, W., Klein, T. & Huber, R. A Time-Encoded Technique for fibre-based hyperspectral broadband stimulated Raman microscopy. *Nature Communications* **6**, 6784, doi:10.1038/ncomms7784 (2015).
- 33 Huber, R., Adler, D. C. & Fujimoto, J. G. Buffered Fourier domain mode locking: unidirectional swept laser sources for optical coherence tomography imaging at 370,000 lines/s. *Opt. Lett.* **31**, 2975-2977, doi:10.1364/OL.31.002975 (2006).
- 34 Yokoyama, H. *et al.* Two-photon bioimaging with picosecond optical pulses from a semiconductor laser. *Opt. Express* **14**, 3467-3471, doi:10.1364/OE.14.003467 (2006).
- 35 Ji, N., Magee, J. C. & Betzig, E. High-speed, low-photodamage nonlinear imaging using passive pulse splitters. *Nat Meth* **5**, 197-202, doi:http://www.nature.com/nmeth/journal/v5/n2/supinfo/nmeth.1175\_S1.html (2008).
- 36 Patterson, G. H. & Piston, D. W. Photobleaching in Two-Photon Excitation Microscopy. *Biophysical Journal* **78**, 2159-2162, doi:http://dx.doi.org/10.1016/S0006-3495(00)76762-2 (2000).
- 37 Débarre, D., Olivier, N., Supatto, W. & Beaurepaire, E. Mitigating Phototoxicity during Multiphoton Microscopy of Live Drosophila Embryos in the 1.0–1.2  $\mu\text{m}$  Wavelength Range. *PLOS ONE* **9**, e104250, doi:10.1371/journal.pone.0104250 (2014).
- 38 Hopt, A. & Neher, E. Highly Nonlinear Photodamage in Two-Photon Fluorescence Microscopy. *Biophysical Journal* **80**, 2029-2036, doi:http://dx.doi.org/10.1016/S0006-3495(01)76173-5 (2001).
- 39 König, K., Becker, T. W., Fischer, P., Riemann, I. & Halhuber, K. J. Pulse-length dependence of cellular response to intense near-infrared laser pulses in multiphoton microscopes. *Opt. Lett.* **24**, 113-115, doi:10.1364/OL.24.000113 (1999).
- 40 Drobizhev, M., Makarov, N. S., Tillo, S. E., Hughes, T. E. & Rebane, A. Two-photon absorption properties of fluorescent proteins. *Nat Meth* **8**, 393-399, doi:http://www.nature.com/nmeth/journal/v8/n5/abs/nmeth.1596.html#supplementary-information (2011).

## Methods (up to 3000 words):

### Time Bandwidth Product in Spectro-temporal Lifetime Imaging via Digitally Sculpted Excitation (SLIDE)

Two photon lifetime imaging in the SLIDE approach places rigorous requirements on the spectro-temporal bandwidth of the light source. The wavelength sweep time  $\Delta T$  is equal to the number of pixels  $n$  times the time between pulses  $\Delta t_i$ , governed by the fluorescent decay time  $\tau_i$ . Considering, for example, 256 horizontal (linescan) pixels and a typical total fluorescent decay time of 10ns, this time calculates to  $\Delta T = 2.56\mu s$ . Assuming a spectral resolution of  $\Delta\lambda_i = 100\text{pm}$  for the diffractive mapping, this means that the light source needs to sweep over  $\Delta\lambda = 25.6\text{nm}$  in  $\Delta T = 2.56\mu s$ . A unique feature in SLIDE is that the spectro-temporal bandwidth scales quadratically with the number of pixels (in linescan):

$$\text{Spectro-temporal bandwidth } M_{ST} = \Delta T \times \Delta\lambda = n^2 \times \Delta\lambda_i \times \Delta t_i$$

A wavelength tuning speed of tens of nm over few microseconds is beyond the reach of conventional tuneable lasers<sup>10,29</sup>. Although very fast tuning speeds can be achieved by chirping a supercontinuum pulse source in a dispersive medium as employed in time stretch techniques, achieving a time span of  $2.56\mu s$  is about three orders of magnitude beyond the reach of available dispersive elements (typically in the ns-regime). Furthermore, the spreading of energy due to the stretching would result in negligible peak powers and would prevent non-linear excitation.

Spectro-temporal stretch via an FDML laser solves this predicament. The FDML laser provides a combination of large spectral span along with microseconds time span and narrow instantaneous linewidth. This novel type of laser has mainly been used for fast optical coherence tomography (OCT)<sup>10,29,30</sup>, semiconductor compressed pulse generation<sup>31</sup> and non-linear stimulated Raman microscopy<sup>32</sup>. Its low instantaneous linewidth allows us to achieve diffraction-limited spatial resolution a feat that is not possible with chirped supercontinuum sources.

#### *Laser: FDML-MOPA*

The FDML-MOPA excitation laser consists of a home-built wavelength-swept FDML laser<sup>10</sup>. The wavelength sweep is accomplished by a fibre Fabry-Pérot-Filter (Lambdaquest) driven at 171kHz. The FDML output is two-times buffered<sup>33</sup> to 342 kHz sweep rate. After the buffer stage, a booster semiconductor optical amplifier (SOA, Innolume SOA-1060-90-Hi-30dB) was installed. The electronic waveforms for the filter and the 50% modulation of the cavity SOA (same model as in booster stage, driven by a Highland Technologies T160 driver) were programmed on an arbitrary waveform generator (AWG, Tektronix AWG7052). The electronic pulses were obtained by differentiating the digital marker outputs of the AWG using a 2.92mm step-to-impulse converter (Entegra Corp.). The obtained optical pulse length was measured to be 65ps (Fig.2E). As amplitude electro-optical modulator (EOM) a 20GHz bandwidth model (Photline NIR-MX-LN-20) was employed in combination with an electronic pulse amplifier (Multilink MTC5515). A high extinction ratio EOM was chosen in order to ensure maximum optical pulse amplification. Potentiometers were inserted to control the DC voltage of the FDML filter, which controls the centre wavelength, and the DC-bias of the EOM, ensuring maximum pulse height. The optical pulses were amplified by home-built ytterbium-doped fibre amplifiers (YDFAs) consisting of three-stages, two core-pumped and one cladding pumped YDFA at 976nm. These home-built YDFAs

were set up similar to described earlier<sup>25</sup>. A 99/1 monitor tap coupler serves for beam monitoring and can also be used in reflection mode for beam alignment using sample light reflections.

### **Picosecond Excitation Pulses for rapid lifetime imaging**

Our fast lifetime imaging capability is possible by the direct analogue recording of the fluorescent lifetime decay and is further enhanced by the higher number of photons generated per pulse by picosecond excitation pulses<sup>25,34</sup>, enabling single pulse per pixel illumination. This has a number of advantages over traditional illumination: (i) A single pulse per pixel leads to a very low effective repetition rate per pixel, equal to the frame-rate (approx. 2kHz). This has been shown to decrease photobleaching and thereby increasing the signal levels<sup>12</sup>. (ii) Longer pulses lead to reduced pulse peak powers at same SNR, thus having the advantage of avoiding higher-than-quadratic effects like photobleaching<sup>35,36</sup> and photodamage<sup>37-39</sup> (scale at orders >2). (iii) The longer pulses are generated by digitally synthesized EO modulation which renders the excitation pattern freely programmable. For example, for optimal detection the pixel rate can be tailored to the fluorescence lifetime of the sample and allows warped (anamorphic) spatial illumination that takes advantage of sparsity to achieve optical data compression. (iv) Longer pulses generate quasi-monochromatic light and this renders the high-speed line-scanning spectral mapping by diffraction gratings possible. (v) The quasi-monochromatic light is optimally compatible with fibre delivery by omitting chromatic dispersion and pulse spreading. The excitation laser presented here is already fully fibre-based, making a future implementation into a multi-photon endoscope straight forward.

### **Wavelength-to-space Mapping**

Upon exiting the single-mode fibre, the light was collimated using an  $f=37$  mm lens followed by a beam-expander ( $f=100$ mm and  $f=150$ mm). This results in a beam diameter of 11.5mm filling the 60x microscope objective aperture. The grating was positioned at a 30° angle, such that the first order was reflected at almost the incident direction in order to minimize ellipticity of the first-order diffraction beam. At 1200 lines/mm the grating only produced a 0 and +1 diffraction order and the first order power was maximized by adjusting the polarization on a polarization control paddle. The grating resolution is calculated to 67pm. This fits well to the instantaneous linewidth of the FDML, which was measured for a single pulse to be 56pm (Extended Fig. 1G). Considering spectral mapping, the 12nm FDML span (cf. Extended Data Fig. 1E) leads to  $12\text{nm}/0.067\text{nm}\approx 180$  discernible pixels, which were oversampled using 256 pulses per sweep, i.e. pixels per line. It is important to note that the applied 12nm sweep span lies well inside most absorption bandwidths<sup>40</sup>. For TPEF imaging, the excitation can be considered monochromatic. A 12nm bandwidth calculates to a  $\sim 140$ fs time-bandwidth limited pulse, which is routinely applied for TPM. In fact, even shorter pulses are used, scaling quadratically in bandwidth. Consequently, even larger FDML spans can be applied in this setup, leading to larger scan fields and fields of view (FOVs) in the future. For simplicity, the excitation can thus be considered almost monochromatic. Any spectral considerations of the excitation serve solely for the purpose of fast, inertia-free beam steering, especially since fluorescence excitation characteristic is independent of the exact excitation wavelength.

### *Microscopy Setup*

Two lenses were used to relay image the beams onto a galvanometric mirror (EOPC) for y-axis scanning. The galvo mirror was driven synchronously, producing 170 lines at 2.012 kHz. A high NA, oil immersion microscope objectives was used (Nikon Plan Apo 60x NA 1.4 oil). The field-of-view (FOV) was determined by inserting a resolution target and recording the reflected excitation light on a CCD camera installed in the microscope, which was sensitive to the 1064nm excitation light (see extended figure 2B). If linearly sampled, the FOV is scanned by a cosine mapping in both axes, so a non-linear mapping is produced. The FOV can be dynamically adjusted using warped sampling or adjusting the swept wavelength and galvo voltages (cf. Fig. 4). A dichroic mirror (Thorlabs DMSP950R) in combination with an additional short-pass optical filter (Semrock FF01-750) transmits the Epi-generated signals to a hybrid Photodetector (HPD, Hamamatsu R10467U-40) with high quantum efficiency (45%). The high time resolution of the HPD in combination with a fast digitizer ( $\sim 3\text{GS/s}$ ) leads to a fast instrument response function (IRF) of only 1026ps, measured by detecting the instantaneous signal of SHG in urea crystals (cf. Extended Data Fig 1H).

### *Digitally synthesized waveforms*

The whole system is driven by an arbitrary waveform generator (AWG, Tektronix AWG7052). This AWG provides all digitally synthesized driving waveforms, driving the FDML laser (Fabry-Pérot Filter waveform and 50% modulation of SOA for buffering), the galvo-mirror and also generates an external sample clock signal for the digitizer. The waveforms are digitally programmed and enable flexibility on the number of pulses per sweep, pulse pattern and enabling the possibility of warped sampling. For very short lifetimes, a higher repetition rate can be employed. The Pollen grain shown in Fig. 2 employed short lifetimes and thus allowed imaging at 176MHz repetition rate.

Fig. 4A-F employ a much lower repetition rate, which lowers the average power on the sample and can avoid photobleaching<sup>12</sup>. However, this advantage – employed here by using only 32 Pulses per 342kHz line-scan – can result in a severe undersampling of the specimen, where important features are missed. This is shown in Fig. 4C. Interestingly, often times the specimen shows regions of higher detail along with regions of lower detail. In nature, this lead to the evolutionary development of foveated sampling in the human retina (and other animals), where more important parts of the image are sampled at higher resolution. Here, we implement this by employing foveated sampling through digitally sculpted waveforms, which efficiently allots the 32 samples to the center of the field-of-view (Fig. 4D-F). A two-fold cosine mapping was applied, effectively increasing the resolution in the center by  $(\pi/2)^2$ , i.e. 2.5-fold. For the digital optical zoom, Figures 4G<sub>1</sub> and 4G<sub>2</sub> were imaged applying 15nm wavelength span, whereas in Fig. 4H and 4I 10nm and 5nm span were used, respectively.

### *Digitizer*

As digitizers, either an oscilloscope (Tektronix DPO71604B) at 3.125 GSamples/s or a streaming ADC card (Innovative Integrations Andale X6GSPS) with synchronously driven sample clock at 3196MHz were employed<sup>25,32</sup>. To ensure sample-accurate fitting, an external sample clock was employed such that the data acquisition runs synchronously to the FDML laser and the pulse modulation. In order to acquire large data sets, a streaming ADC in combination with a RAID-SSD array was employed to store the data and process in post acquisition.

### Flow cytometry

In the flow cytometry recording, the flow-rate was set by two fundamental properties, namely the fluorescence lifetime and the imaging diffraction limit. The lifetime limits the repetition rate to  $\sim 100\text{MHz}$ , while the diffraction limit is sampled at  $\sim 380\text{nm}$ . Consequently, we employed  $88\text{MHz}$  repetition rate at 256 pulses per  $2.92\mu\text{s}$  linescan rate and  $100\mu\text{m}$  field-of-view. The flow rate was equally set to sample each line at  $380\text{nm}$ , i.e.  $380\text{nm}/2.92\mu\text{s}=0.13\text{m/s}$ . The scale bars in the flow cytometry images were generated using the known  $10\mu\text{m}$  size of the Red-species bead to calibrate the actual flow speed. The Red bead was sampled with 18 lines, calculating to a line spacing of  $556\text{nm}$ . Using the line scan rate of  $342\text{kHz}$ , this calculates to a flow speed of  $\sim 0.2\text{m/s}$ . At  $100\mu\text{m}$  field-of view and  $10\mu\text{m}$  average particle size, this corresponds to the possibility of imaging up to 200,000 particles per second via 2P-FLIM. In the future, a multi-threaded GPU approach in combination with more efficient lifetime extraction (cf. Fig. 3C) can process and visualize this data in real-time<sup>30</sup>. By further combining this imaging setup with GPU-based machine learning, this setup can lead to high-speed, high-throughput cell classification and screening<sup>21</sup>.

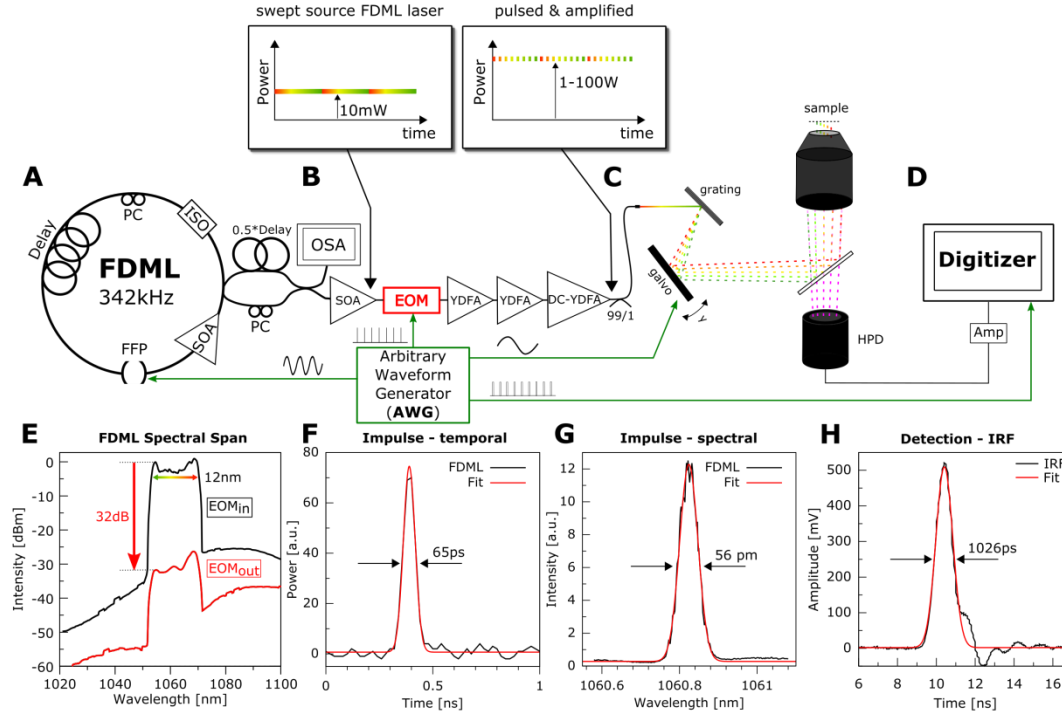
### Data Processing

For precise measurement, a deconvolution with the IRF was conducted in order to extract the fluorescent lifetimes. However, this is time consuming, so for faster processing and qualitative results a tail-fitting algorithm was used. Often time, different species need to be discerned so a qualitative value is sufficient. In Fig. 3, a direct signal processing approach was conducted, not requiring any fitting and thus being very fast. In the *Euglena* algae cell images (Fig. 3C<sub>1,2</sub>), the first 1ns of the decay signal was integrated and used for the red image channel in order to visualize the rapidly decaying chlorophyll autofluorescence. For the green channel, the Nile Red lipids were visualized by integrating the signal from 2-8ns, i.e. later in the decay curve. This resulted in a clear molecular contrast based on fluorescence lifetime. For all images, the data was processed and images created in LabVIEW. The 2P-FLIM images were generated as HSL-images, where Hue was given by the lifetime-values, lightness by the integrated TPEF signal and constant saturation. For the TPEF images, the “Red Hot” look-up table was applied in ImageJ. The plots were generated in GNUPlot and the figures produced using Inkscape.

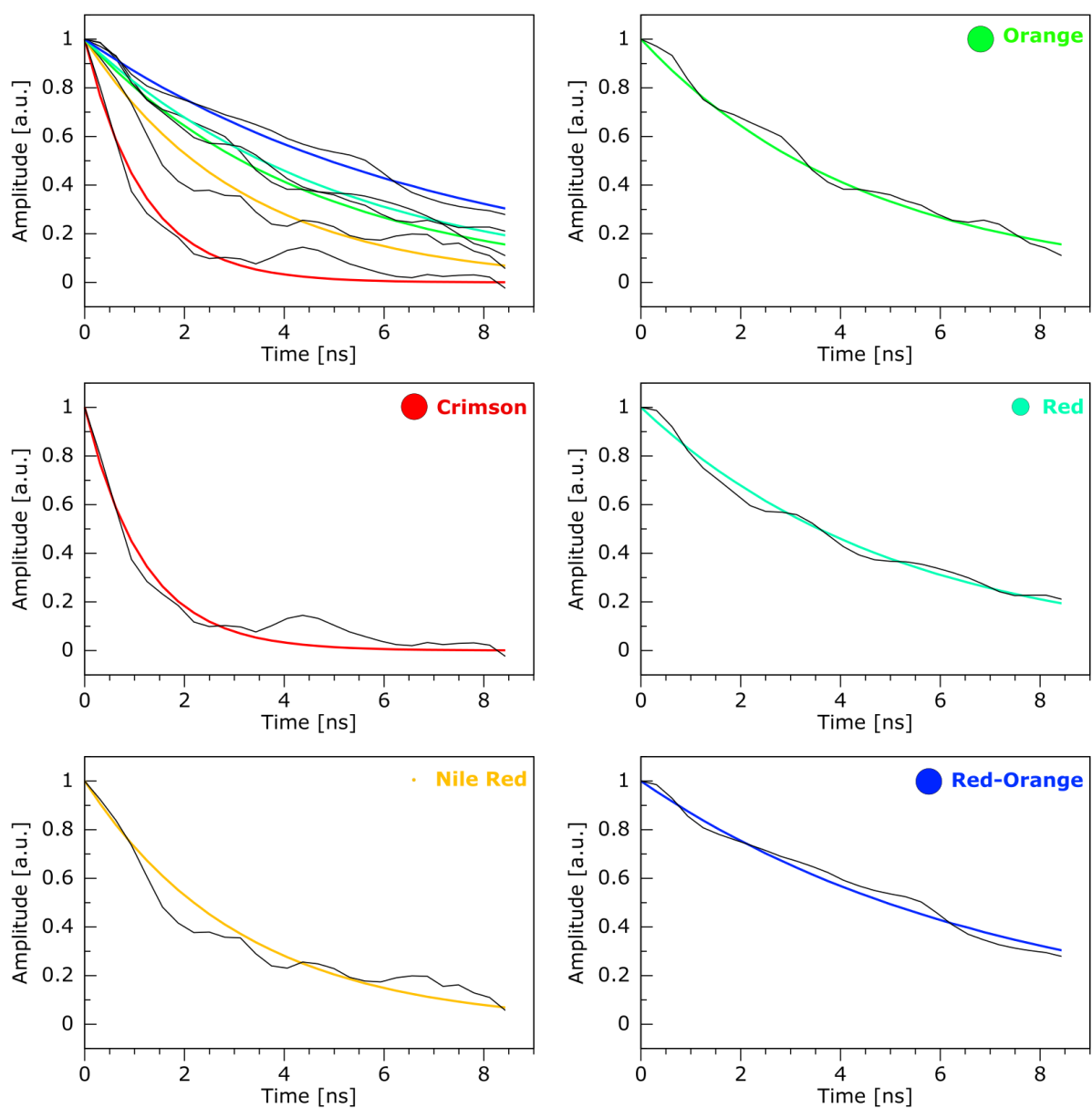
### Samples

The Pollen grain samples were ordered from Carolina (B690 slide) and the acridine orange stained *convallaria majalis* (lily of the valley flower stem) from Lieder GmbH, Germany. The fluorescent beads were ordered from ThermoFisher Scientific (# F8825, F8839, F8841, F8843, and F21012).

## Extended Data

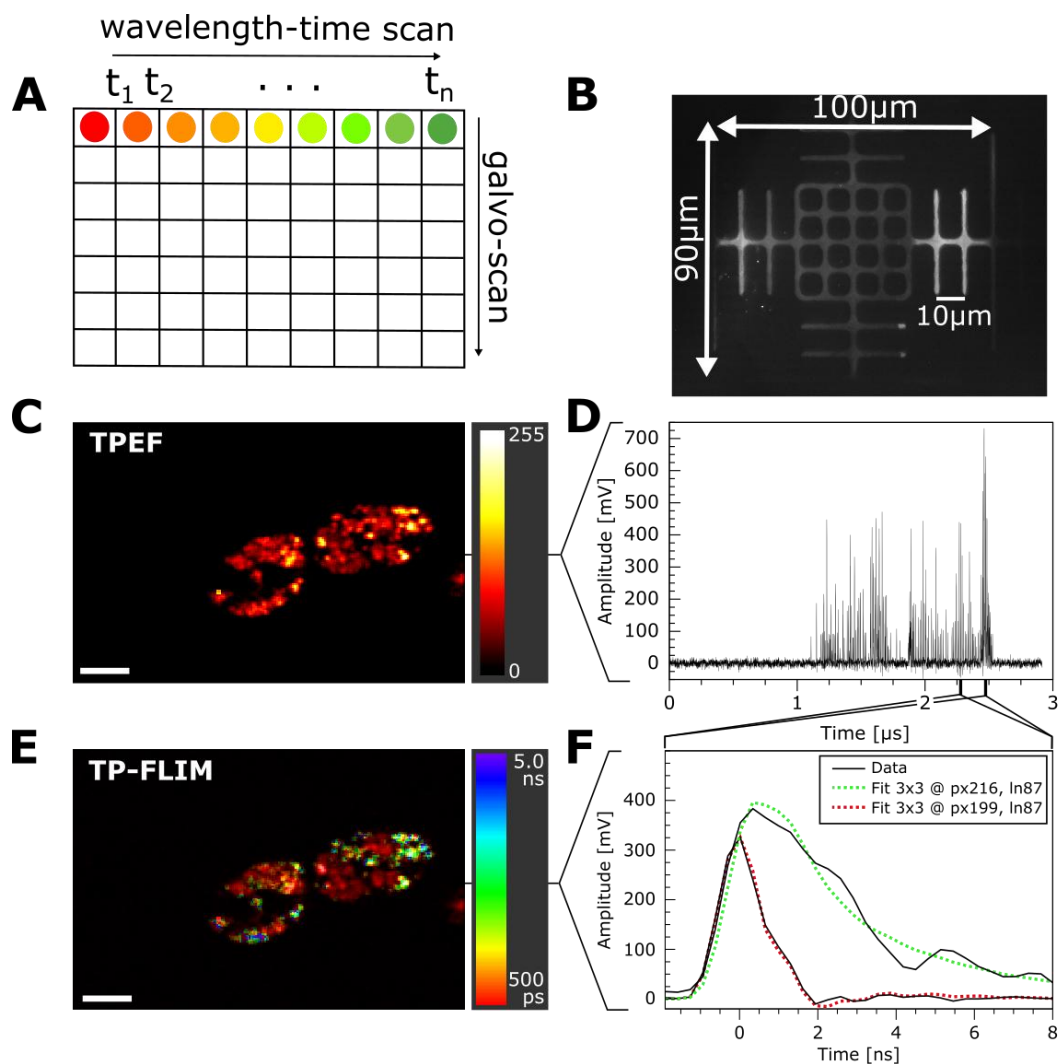


**Extended Data Figure 1 Setup of the Spectro-temporal Lifetime Imaging by digitally sculpted excitation (SLIDE) system.** (A) The light source consists of a wavelength swept FDML laser<sup>10</sup> at 1060nm ( $\pm 6$ nm) and 342 kHz sweep repetition rate (PC: Polarization Controller, SOA: semiconductor optical amplifier, ISO: Isolator, FFP: Fiber Fabry-Pérot Filter, OSA: optical spectrum analyzer). (B) The boosted output is modulated by typically 256 impulses of short temporal width (65ps) by an electro-optical modulator (EOM). The impulses are digitally synthesized on an arbitrary waveform generator (AWG), which also drives the FDML laser. To enable non-linear excitation, these pulses are amplified to high instantaneous powers by two core-pumped ytterbium-doped fibre-amplifiers (YDFAs) and a double-clad power amplifier (DC-YDFA). A 99/1 tap coupler serves as monitor port. (C) Spectral line-scanning is achieved by a diffraction grating. The y-axis is scanned by a synchronously driven galvo scanner. The driving signal is also generated on the AWG. A high numerical aperture (NA) objective focuses the excitation light on the sample and collects the epi-generated fluorescence signal. A dichroic filter directs only non-linear signals on a fast hybrid photodetector (HPD), connected to a transimpedance amplifier and a fast digitizer (D). The sample clock of the digitizer can also be synchronized to the excitation by a sample clock signal from the AWG. (E) A wavelength span of 12nm is used for spectral scanning. The EOM modulator achieves a high extinction ratio ( $\sim 30$  dB optical). (F) The recorded temporal pulse width achieved with the EOM is 65ps. (G) High-resolution pixel mapping is possible due to the narrow instantaneous linewidth of the pulsed FDML laser pulses measured to 56pm. (H) The instrument response function (IRF) of the detection was determined by SHG in urea crystals to 1026ps FWHM.



Extended Data Figure 2 Raw Data to flow cytometry fluorescent beads measurement. Shown are curves of the five different beads species. The raw data of the fluorescent decay signals are plotted together with their fitted exponential-decays, which were then used for colouring. The raw-data is taken from a single pixel, after a 9x9 pixel box blur filter was applied.





Extended Data Figure 3 Two-Photon Excited Fluorescence (TPEF) and Two-Photon Lifetime (2P-FLIM) images of *Euglena gracilis* algae. (A) The schematic shows the beam-scanning concept, where the x-axis is scanned by a wavelength-time scan and the y-axis scanned by a galvo mirror. (B) The experimentally realized field-of-view as measured by reflection off a resolution test target. This image was recorded by the CCD camera in the microscope and shows the  $100 \times 90 \mu\text{m}^2$  field-of-view (FOV) (resolution target has  $10 \mu\text{m}$  pitch). (C) SLIDE image of a *Euglena gracilis* algae cell, which provides endogenous two-photon fluorescence of chlorophyll at 1060nm and Nile Red stained lipids. This unaveraged image was acquired at 2.012 kHz frame-rate ( $497 \mu\text{s}$  recording time). A 3x3 box blur filter was applied to the image and achieves peak SNR of 490 for 30mW average power on the sample. The raw-data time-trace of a single-line is shown in (D), recorded in  $2.92 \mu\text{s}$ . For this line-rate of 342kHz a horizontal 256 pulses were programmed resulting in a pixel-rate of 88MHz. By fitting an exponential-decay curve to every pixel, convoluted with the IRF, a Two-Photon lifetime image (TP-FLIM) is generated. The obtained TP-FLIM image is colour-coded with lifetimes from 500ps to 5000ps. The chloroplasts have a shorter lifetime (red) and can clearly be distinguished from the green and blue Nile Red lipids, which have longer fluorescence lifetimes. (F) Time-domain lifetime data of a single pixel of Nile Red and chlorophyll, together with the fitted convolution model. A 3x3 average (box blur) was applied to the time-domain lifetime data before fitting.